NJC

Accepted Manuscript

This is an *Accepted Manuscript*, which has been through the Royal Society of Chemistry peer review process and has been accepted for publication.

Accepted Manuscripts are published online shortly after acceptance, before technical editing, formatting and proof reading. Using this free service, authors can make their results available to the community, in citable form, before we publish the edited article. We will replace this *Accepted Manuscript* with the edited and formatted *Advance Article* as soon as it is available.

You can find more information about *Accepted Manuscripts* in the **Information for Authors**.

Please note that technical editing may introduce minor changes to the text and/or graphics, which may alter content. The journal's standard **Terms & Conditions** and the **Ethical guidelines** still apply. In no event shall the Royal Society of Chemistry be held responsible for any errors or omissions in this *Accepted Manuscript* or any consequences arising from the use of any information it contains.

NJC

PAPER (or FOCUS or PERSPECTIVE)

Light absorption and hole-transport properties of copper corroles: from aggregates to a liquid crystal mesophase.

Di Gao,[a] Judicaelle Andeme Edzang,[b] Abdou Karim Diallo,[b] Thibault Dutronc,[c] Teodor Silviu Balaban,[a] Christine Videlot-Ackermann,*[b] Emmanuel Terazzi*[c] and Gabriel Canard*[b]

The synthesis of the corrole-based liquid crystal phase **CorLC** is described together with its full characterization by a combination of Polarised Optical Microscopy (POM), ThermoGravimetric Analysis (TGA), Differential Scanning Calorimetry (DSC) measurements and Small-Angle X-Ray Diffraction (SA-XRD) which shows that **CorLC** has an hexagonal columnar organization at room temperature. The light absorption and hole-transport properties of the mesophase **CorLC** is compared with the ones featured by assemblies of its parent *meso* triaryl (**Cor1**) and *per*-aryl (**Cor2**) derivatives. J-Aggregates are changed into H-aggregates when the intermolecular distance is increasing with the peripheral steric hindrance producing lower hole-transport properties.

Introduction

The highly versatile optical, electronic and photophysical properties of porphyrin and phthalocyanine derivatives has led to their large application in the fields of organic electronics and optoelectronics.[1] In this regard, their ability to produce large assemblies or aggregates is particularly employed to construct organized and high light-absorbing materials displaying efficient charge and/or exciton transport properties that are essential in the preparation of organic solar cells[2] or photoconductors.[3] Among the different supramolecular tools that are used to build self-organized porphyrin and phthalocyanine systems, their incorporation in liquid crystal (LC) phases[4] is attractive since the morphology and orientation of LC thin films can be controlled to obtain large area and defect free devices.[5] For example, an exciton diffusion length longer than 12 nm has been measured in a nematically organized porphyrin layer[6] while a field-effect mobility of 0.7 cm^2 V^{-1} s^{-1} was exhibited by an Organic Field Effect Transistor (OFET) incorporating a liquid crystalline copper phthalocyanine.[7]

Corrole and its metal complexes are currently attractive members of the porphyrinoid family since their syntheses[8] and functionalizations[9] have been extensively developed during the last fifteen years and are thus amenable to gram-scale synthesis, sometimes essential for developing devices. Consequently, corrole derivatives are employed in many research areas including catalysis,[10] sensors[11] or medicine.[12] Nevertheless, very few reports concern the preparation and characterization of large corrole-based assemblies[13] and their incorporation into electronic devices.[14] We report here the synthesis and full characterization of a copper corrole-based liquid crystal mesophase **CorLC** (Scheme 1). Its supramolecular organization was studied by UV/Visible spectroscopy and was compared to the ones produced by aggregates of its parent *meso* triaryl (**Cor1**) and *per*-aryl (**Cor2**) derivatives (Scheme 1). The hole-transport properties of these three compounds were additionally measured through their incorporation in OFETs.

Results and discussion

Synthesis of the mesogen CorLC.

The liquid crystal **CorLC** was prepared in four synthetic steps starting from the copper(III) *meso*-tris(*p*-methoxyphenyl)corrole **Cor1** (Schemes 1 and S1, ESI†).[15] The full bromination of β-positions followed by a Suzuki cross-coupling procedure afforded the *per*-aryl substituted copper corrole **Cor2** as previously reported.[16] A demethylation using standard conditions afforded the *per*-aryl complex substituted by eleven *p*-hydroxyphenyl groups in 44% yield without any noticeable removal of the copper ion. It has to be noted that this latter derivative is enough soluble in sufficiently polar media in order to be purified and characterized. The expected compound **CorLC** was prepared in a yield of 23% by the subsequent condensation of an excess of the benzyl chloride

derivative **1** in basic conditions. Its purity was confirmed by its ^{1}H NMR spectrum and by its MALDI-TOF spectrum showing only its molecular peaks and the corresponding sodium adduct (ESI†). We note here that if a reaction has to be performed more than tenfold on the same substrate, without allosteric effects, it is remarkable that the overall yield is in the two digit region.
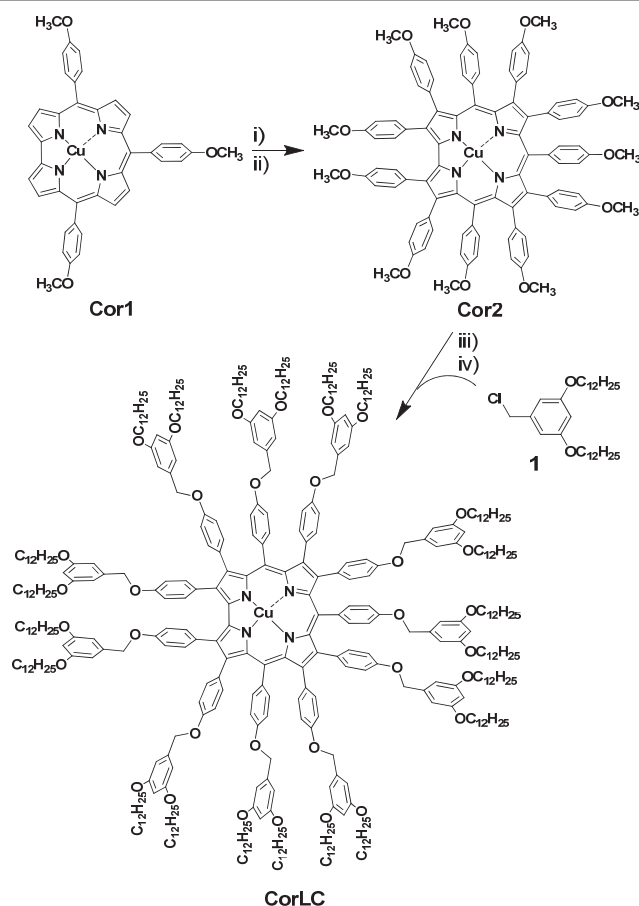

Scheme 1 Synthesis of the liquid crystal corrole **CorLC**. i) a) Br$_2$, pyridine, CHCl$_3$; b) NaS$_2$O$_5$, H$_2$O (45%). ii) Pd$_2$(dba)$_3$, K$_2$CO$_3$, *p*-H$_3$CO-C$_6$H$_4$-B(OH)$_2$, toluene (71%). iii) BBr$_3$, CH$_2$Cl$_2$ (44%). iv) K$_2$CO$_3$, DMF (23%).

Thermal behaviour of CorLC.

The thermal behavior of **CorLC** was studied by a combination of Polarised Optical Microscopy (POM), ThermoGravimetric Analysis (TGA), Differential Scanning Calorimetry (DSC) measurements and Small-Angle X-Ray Diffraction (SA-XRD) (Fig. 1, Fig. S1, S2 and S3, ESI†). The TGA measurement indicates that the compound is stable up to 300 °C (Fig. S1, ESI†). Temperature dependent POM observations showed a fluid and birefringent texture that is typical of the occurrence of a liquid-crystalline organization. This texture does not show any significant changes until the isotropisation occuring at 103 °C i.e. a transition from the liquid crystalline phase to the standard liquid state (I). Upon cooling, this phase transition is reversible and occurs at 95 °C (i.e. with a small hysteresis). Notably, the liquid crystal phase remains birefringent and fluid at room temperature. Cooling down the isotropic liquid sample at very low speed (0.1 °C·min^{-1}) forms the liquid crystalline

phase characterized by a fan texture that strongly suggests that the compound self-organizes in a columnar hexagonal (Col$_h$) liquid crystalline phase (Fig. 1a). This preliminary result was confirmed by DSC (Fig. 1b). The solid complex **CorLC** was transformed to the Col$_h$ mesophase through a broad first order transition (-30 °C, ΔH = 80.4 kJ·mol^{-1}, ΔS = 330.5 J·mol^{-1}·K^{-1}) that preceded a second first order transition (103.4 °C, ΔH = 22.1 kJ·mol^{-1}, ΔS = 58.8 J·mol^{-1}·K^{-1}) of the Col$_h$ phase into the liquid isotropic state I.
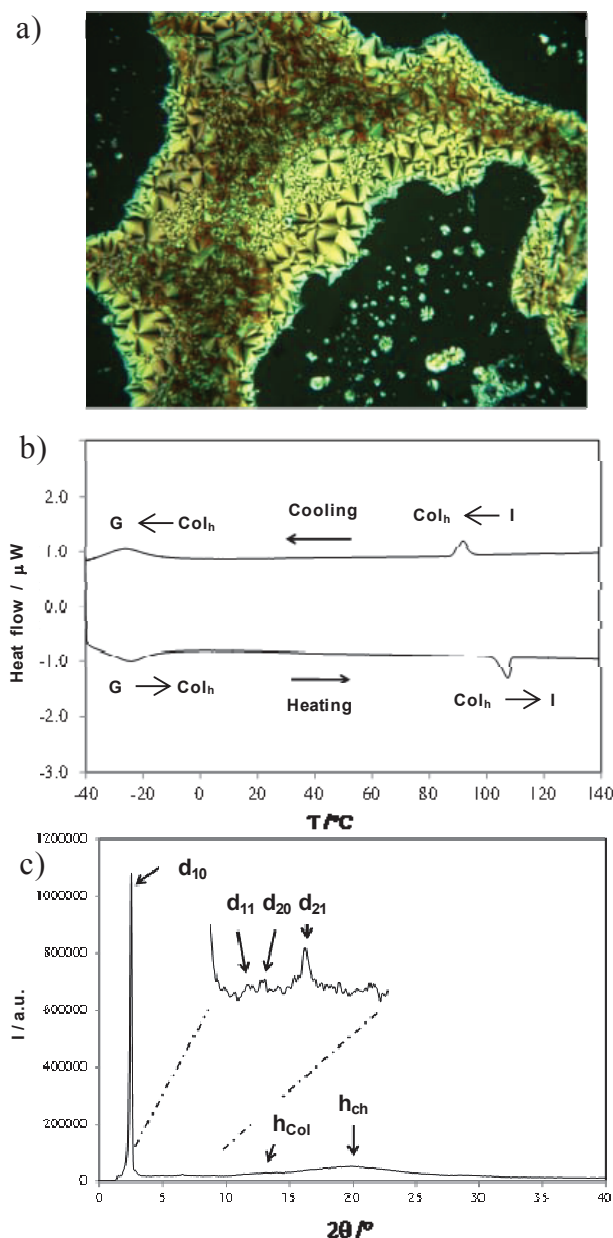
Fig. 1 (a) Optical texture observed by the POM of **CorLC** in the Col$_h$ mesophase at 90 °C after cooling from the isotropic liquid. (b) DSC trace of **CorLC** recorded at 5 °C/min (second heating and cooling). (c) SA-XRD profile in the liquid crystalline phase and associated indexation of **CorLC** at 30 °C.

Structure of the CorLC mesophase.

Temperature-dependent SA-XRD patterns of **CorLC** were recorded in the 20-140 °C temperature range. The presence of a large and diffuse signal at approximately 4.5 Å (h_{ch}), which was associated with the liquid-like molten chains confirmed the fluid-like nature of the mesophase. Short acquisition times (i.e. 10 min per scan) allowed to detect a very weakly temperature-dependent sharp and intense signal at low angle in the 20-100 °C temperature range. A longer acquisition time at 30 °C (i.e. 24 hours) revealed the presence of three additional very weak reflections in the low angle region (Fig. 1c)). These four sharp reflections were indexed as $(hk) = (10), (11), (20), (21)$ (squared spacing ratios $h^2 + k^2 + hk = 1, 3, 4, 7$; see Fig. S2, ESI†) confirming the formation of a Col_h arrangement suggested by the POM observation (plane group *p6* or *p6mm*).[17] A unit cell parameter of $a = 41.1$ Å and a cross-sectional area of $S = 1462$ Å^2 were thus deduced from this last measurement. The pattern recorded at 30 °C shows a second broad reflection (h_{Col}) located at about 7 Å partially overlapping the first one corresponding to the molten aliphatic chains (i.e. h_{ch}). The separation of these two broad signals by fitting them with Gaussian functions (Fig. S3, ESI†) allowed to accurately determine the value of $h_{Col} = 6.86$ Å. Making the assumption that h_{Coh} corresponds to the separation between the complexes within a column, we thus calculated a volume of $V = S \cdot h_{Col} = 10029$ Å^3 for an hexagonal columnar unit cell. Taking into account a realistic density of $d = 1.0$ g·cm^{-3} in the mesophase,[17d] we estimated that the number of complexes **CorLC** per unit cell Z amounts to 1 according to equation (1) where N_{av} is the Avogadro's number, MM_m is the molecular weight of the molecule in g·mol^{-1}, and V is the volume of the unit cell in Å^3.[17d] The liquid crystalline supramolecular organization of complex **CorLC** should thus be considered as a bidimensional long-ranged network with a rather disorganized third direction (i.e. along the column axis) that is typical of Col_h organizations. This kind of organization is commonly observed in mesophases produced by porphyrin- and phthalocyanine-based discotic derivatives bearing multiple long alkyl chains.[4] For example, a Col_h organization was also displayed by a porphyrin bearing four peripheral mesogenic bis-dodecyloxy aryl groups which are similar to those born by **CorLC**.[4b]

$$(1) \quad Z = (d.N_{AV}.V.10^{-24}) \div MM_m = 0.94 \sim 1$$

Aggregation properties of Cor1, Cor2 and CorLC.

Copper *meso*-triarylcorroles are known to show *hyper* electronic spectra that are strongly sensitive to the nature of the *meso*-substituents that are involved in phenyl-to-Cu($d_{x^2-y^2}$) charge transfers and contribute to the main Soret band peak.[18] This orbital interaction is due to and increases with the saddling of the macrocycle which is reinforced by the introduction of bulky β-aryl groups.[16,19] This effect is here illustrated by the UV/Visible spectra of diluted dichloromethane solutions of

Cor1, **Cor2** and **CorLC** (Fig. 2). The *per*-aryl substitution produces the broadening of the Soret band which is red-shifted from 433 nm in the spectrum of **Cor1** to 463 nm and 464 nm in the respective electronic spectra of **Cor2** and **CorLC**. On the other side, the replacement of the methyl groups of **Cor2** by benzyl substituents in **CorLC** does not induce any significant change in the location of the B and Q bands and on the shape of the UV/visible spectrum. This similarity is due to the equivalent electron-donating properties of these two groups and shows that the concomitant introduction of 11 additional aryl groups and 21 peripheral alkyl chains does not produce any supplementary distortion of the aromatic corrole ring.

Thin solid films of **Cor1**, **Cor2** and **CorLC** were prepared by the slow evaporation of their respective dichloromethane solutions. The formation of aggregates is illustrated by the broadening of the resulting electronic spectra that gives, in addition, insights of the relationship between the corroles substitutions and their supramolecular organizations (Fig. 2).
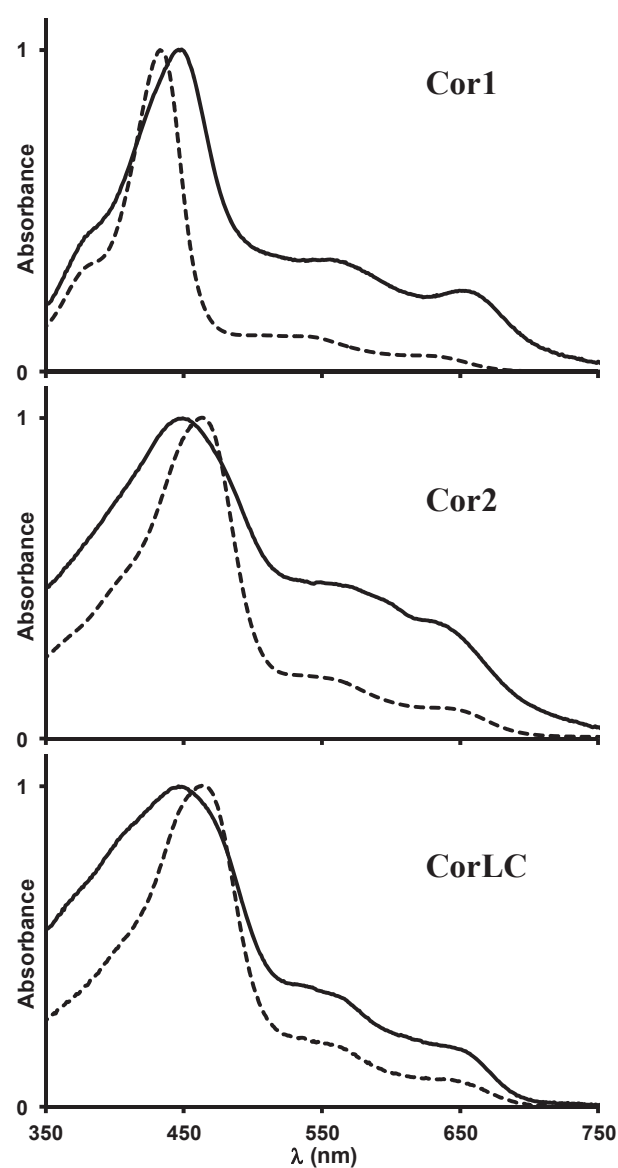
Fig. 2 Normalized UV-Visible absorption of diluted dichloromethane solutions (dashed lines) and thin solid films (solid lines) of **Cor1**, **Cor2** and **CorLC**.

The band maxima are red-shifted by ca 15 nm when assemblies of **Cor1** are produced because of the probable formation of J-aggregates. This supramolecular architecture is commonly observed in the single crystal X-ray structures of copper *meso*-triarylcorrole derivatives where corrole assemblies are formed thanks to, among others, an intermolecular interaction between the *meso*-aryl group of one complex with the metallic centre of the adjacent one producing short inter-macrocycle distances.[20] On the other side, the *per*-aryl substitution of **Cor2** and **CorLC** induces the formation of H-aggregates as evidenced by the ca 20 nm blue-shift of their Soret band maxima (Fig. 2). The peripheral sterical hindrance of **Cor2** combined with the multiple intermolecular interactions between alkyl chains in the LC phase **CorLC**, inhibits the direct participation of the copper ion in the supramolecular organization and thereby allows the formation of a different intermolecular packing. The formation of H-assemblies along the column axis is in accordance with the Col$_h$ organization of the **CorLC** mesophase (see below).

Hole-transport properties of Cor1 and Cor2.

To further study the physico-chemical properties of **Cor1**, **Cor2** and **CorLC** assemblies, their charge-transport properties were investigated through their incorporation in OFETs. Bottom-gate thin-film transistors with bottom electrode contacts were fabricated to realize so-called BGBC (Bottom-Gate Bottom-Contact) devices. Linear channel lengths (L = 25 or 50 µm) were realized by vacuum evaporation of gold through a shadow mask directly on the gate. To complete the device structure, the depositions of the active layers were achieved by drop-casting of dichloromethane solutions (or liquid **CorLC**) onto the surface of linear BGBC devices. All measurements were performed in air and at room temperature. Even if numerous OFETs were prepared for each derivative, only the two best results obtained among the operating transistors are presented herein.

A field effect transistor activity was observed for **Cor1** and **Cor2**-based assemblies by applying a negative drain and negative gate voltages in order to operate in the accumulation mode. These results demonstrate that **Cor1** and **Cor2** behave as p-type semiconductors in air as shown by the typical output characteristics of a **Cor1**-based OFET on Si/SiO$_2$ substrate under negative and positive voltages (Fig. 3a and Fig. 3b). Under negative gate voltages, the successive increase of the drain current indicates that the BGBC device based on **Cor1** operates as an accumulation mode p-channel device (Fig. 3a). The transport of positive carriers is confirmed by the depletion mode under positive voltages (Fig. 3b). In the depletion mode, carriers are driven away from the semiconductor interface, which leads to a decrease of the drain current. The field effect mobility (μ), threshold voltage (V_T) and on/off ratio (I_{on}/I_{off}) of the most efficient OFETs incorporating **Cor1** and **Cor2** are summarized in Table 1 (All results are presented in Table S1, ESI†). The highest field effect mobility in the saturation regime at V_D = -90 V was extracted for **Cor1** and gives a value of 1.36×10^{-6} cm^2/V.s^{-1} together with a threshold voltage V_T of +14.8 V and an on/off ratio of 24.5. The increasing sterical hindrance of the peripheral substitution of **Cor2** probably produces a lower mobility of 1.32×10^{-7} cm^2/V.s^{-1} together with

a threshold voltage V_T of +38.5 V and an on/off ratio of 10. All devices incorporating **CorLC** failed to give charge-transport properties. Identical results were obtained when an hydrophobic substrate Si/SiO$_2$ modified by a grafted self-assembly monolayer of long alkyl chains was used to induce the homeotropic alignment of the **CorLC** discotic molecules.[21] Although thin films were cast as such, or with an annealing step, these failed to improve the microstructural order for achieving more efficient charge transport properties in **Cor1**, **Cor2** and **CorLC** thin films. However, these functional transistors are the first examples of OFETs using corrole derivatives as active layers and the variation of their low efficiencies are still illustrating the impact of the peripheral substitution on the corroles supramolecular organization.
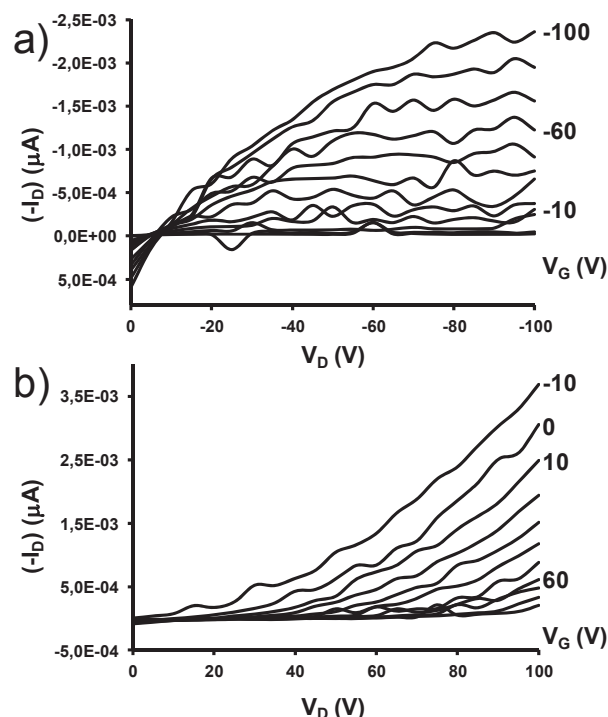
Fig. 3 Output characteristics of an OFET incorporating **Cor1** under a) negative and b) positive voltages.

Table 1: Field effect mobilities (µ), threshold voltages (VT) and on/off ratio (I_{on}/I_{off}) of corrole-based OTFT devices.

	μ (cm^2.V^{-1}.s^{-1})	V_T (V)	I_{on}/I_{off}
Cor1	$1,36 \times 10^{-6}$	+14,8	24,5
Cor2	$1,32 \times 10^{-7}$	+38,5	~10

Conclusions

We described herein the synthesis and full characterization of the first example of a corrole-based liquid crystal mesophase (**CorLC**). This mesophase features, at room temperature, an hexagonal columnar organization combined with an H-arrangement of the discotic chromophores producing a blue shifted light absorption. This study shows that the introduction of numerous peripheral groups on copper corroles tunes their

aggregation modes and their hole-transport properties. Since the copper ion can be removed using mild experimental conditions,[22] **CorLC** can be used to prepare liquid crystal phases incorporating other metallic centers such as Co(III)[11a] and Mn(III)[14a] that are already applied in the fields of sensors.

Experimental section

General Remarks

All reagents were purchased from Acros, Alfa Aesar or Aldrich and were used without further purification unless otherwise stated. Toluene was distilled from sodium and benzophenone. Dichloromethane, hexane and *n*-heptane were distilled from calcium hydride. Dichloromethane stabilized by methanol was used during the preparation of OFETs. Silica gel plates Merck 60 F254 were used for Thin Layer Chromatography (TLC). Silica gel 60 (230-400 mesh) was used for preparative column chromatography. Flash column chromatography was performed on silica gel 60 (230-400 mesh). (3,5-bis(dodecyloxy)phenyl)methanol,[23] **Cor1**[15] and **Cor2**[16a] were prepared and purified according to literature procedure.

Spectroscopic and analytical measurements

^{1}H Nuclear Magnetic Resonance (NMR) spectra were recorded on a Bruker Avance 400 Ultrashield NMR spectrometer. Chemical shifts are given in ppm relative to residual peaks of chloroform (δ = 7.26 ppm), DMSO-d_6 (δ = 2.50 ppm) or THF-d_8 (δ = 1.73 and 3.58 ppm).

UV/Vis absorption spectra were measured with a Shimadzu UV-2401 (PC) instrument or with a Varian Cary 1E spectrophotometer.

Pneumatically-assisted electrospray (ESI-MS) mass spectra were recorded from 10-4 M solutions on an Applied Biosystems API 150EX LC/MS System equipped with a Turbo Ionspray source. High Resolution Mass Spectrometry (HRMS-ESI) analyses were performed on a QStar Elite (Applied Biosystems SCIEX) spectrometer or on a SYNAPT G2 HDMS (Waters) spectrometer. These two instruments are equipped with an electrospray ionization source and were used within the positive ion mode and with a capillary voltage set at +5500 V. MALDI-TOFF mass spectra were obtained on a Voyager Instrument from Applied Biosystems either with anhydrous glycerol, HABA [2'-(4-hydroxyphenylazo)benzoic acid], or 1,8,9-anthracenetriol (dithranol) matrices.

Liquid crystals analyses.

TGA was performed with a Seiko TG/DTA 320 thermogravimetric balance (under N_2). DSC traces were recorded with a Mettler Toledo DSC1 Star Systems differential scanning calorimeter from 3 to 5 mg samples (5 °C min^{-1}, under N_2). Characterization of the mesophases was performed with a Leitz OrthoplanPol polarizing microscope with a Leitz LL 20x/0.40 polarizing objective and equipped with a Linkam THMS 600 variable temperature stage. The SA-XRD patterns were obtained with three different experimental setups, and in all cases, the crude powder was filled in Lindemann capillaries of 1 mm diameter. (1) A STOE STADI P transmission powder diffractometer system using a focused monochromatic Cu-Kα_1 beam obtained from a curved germanium monochromator (Johann-type) and collected on a curved image-plate position sensitive detector. A calibration with silicon and copper laurate standards, for high- and low-angle domains, respectively, was preliminarily performed. Sample capillaries were placed in the high-temperature attachment for measurements in the range of desired temperatures (from 20 to 160 °C), for which the sample temperature was controlled within 0.05 °C. The exposure times were varied from 1 to 6 h, depending on the specific reflections being sought (weaker reflections obviously taking longer exposure times).

OFET preparations and studies

Cor1, **Cor2** and **CorLC** were dissolved in CH_2Cl_2 to a concentration of ca 5.10^{-3} M. The Bottom-Gate Bottom-Contact (BGBC) configuration was used for the OTFT devices. Highly n-doped silicon wafers (gate), covered with thermally grown silicon oxide SiO_2 (3000 Å, insulator layer), were purchased from Vegatec (France) and used as bottom-gate substrates. The capacitance per unit area of silicon dioxide dielectric layers was 1.2×10^{-8} F/cm^2. The gold (Au) source and drain electrodes (channel length L = 25 or 50 μm, channel width W = 1 mm) were evaporated directly on SiO_2 layer prior the organic deposition through a shadow mask. Solutions of **Cor1**, **Cor2** and **CorLC** (or pure liquid **CorLC**) were deposited by drop-casting to form the organic active layers in OTFT devices through a dropwise addition of 20-40 µL volumes onto the devices surfaces. Such volume covered entirely the channel of one OTFT and beyond. After the organic solution deposition, the devices were left overnight in ambient condition in order to remove residual solvent prior electrical measurements. A post-annealing step from 50 to 80°C was applied to all devices in order to increase the microstructural order of thin films. Current-voltage characteristics were recorded at room temperature under ambient conditions with Hewlett-Packard 4140B, or 4145A, pico-amperemeter-DC voltage sources. The source-drain current (ID) in the saturation regime is governed by the equation (2):

$$(2) \quad (I_D)_{sat} = (W/2L) \; C_i \mu (V_G - V_t)^2$$

Ci is the capacitance per unit area of the gate insulator layer, VG is the gate voltage, Vt is the threshold voltage, and µ is the field-effect mobility. The on/off ratio values were determined from the I-V transfer plots under a constant drain-source voltage VD = -100 V.

Organic syntheses.

Compound 1 : (3,5-bis(dodecyloxy)phenyl)methanol (5.00 g, 10.5·mmol) was dissolved in dry CH_2Cl_2 (50 mL) and DMF (50 µl) was added under a nitrogen atmosphere. A solution of $SOCl_2$ (1.87 g, 15.7·mmol) in dry CH_2Cl_2 (50 mL) was added dropwise over a period of 1 hour. The reaction mixture was stirred at room temperature for 24 hours, evaporated to dryness and dried under vacuum to provide **1** as a white solid (5.15 g, 10.4 mmol, 99%). 1H NMR (400 MHz, CDCl$_3$): δ=0.91 (t, ^3J(H, H) = 6.6 Hz, 6H), 1.29-1.50 (m, 36H); 1.75-1.80 (m, 4H), 3.95 (t, ^3J(H, H) = 6.5 Hz, 6H), 4.52 (s, 2H), 6.42 (t, ^4J(H, H) = 2.5 Hz, 1H), 6.53 (d, ^4J(H, H) = 2.5 Hz, 2H). ESI-MS (CH_2Cl_2/MeOH 9:1): m/z: (M+.): 495.5; calcd for $C_{31}H_{56}ClO_2^+$: 495.4.

Cu^{III} undeca-(4-hydroxyphenyl)corrole: A 1M solution of BBr$_3$ in CH_2Cl_2 (10 mL, 10 mmol) was added to a solution of **Cor2** (45 mg, 29.6 µmol) in CH_2Cl_2 (6 mL) which was stirred at 0 °C for 15 min. The mixture was kept at 0 °C for 1 h and then stirred at room temperature for 3 days before CH_2Cl_2 (20 mL) and CH_3OH (10 mL) were added together with an aqueous saturated solution of NaHCO$_3$ (35 mL). The crude compound was precipitated by pouring the reaction mixture into water (100 mL). The precipitates were filtered and purified by chromatography on silica gel (CH_2Cl_2/CH_3OH, 5:1) to afford **3** as a brown powder (18 mg, 13.1 µmol, 44%). R$_f$ = 0.11 (CH_2Cl_2/CH_3OH, 4:1). ^{1}H NMR (400 MHz, THF-d_8, 25 °C): δ= 7.85 (s, 2H, Ar-O*H*), 7.83 (s, 3H, Ar-O*H*), 7.63 (s, 2H, Ar-O*H*), 7.53 (s, 2H, Ar-O*H*), 7.47 (s, 2H, Ar-O*H*), 6.94 (d, ^3J(H, H) = 8.4 Hz, 2H, Ar-H), 6.76 (d, ^3J(H, H) = 7.9 Hz, 4H, Ar-H), 6.66 (d, ^3J(H, H) = 8.4 Hz, 4H, Ar-H), 6.40 (d, ^3J(H, H) = 7.6 Hz, 8H, Ar-H), 6.40 (d, ^3J(H, H) = 8.0 Hz, 4H, Ar-H), 6.27 (d, ^3J(H, H) = 8.5 Hz, 4H, Ar-H), 6.09 (m, 8H, Ar-H), 6.03 (d, ^3J(H, H) = 8.6 Hz, 4H, Ar-H), 5.96 (d, ^3J(H, H) = 7.5 Hz, 4H, Ar-H), 5.93 ppm (d, ^3J(H, H) = 8.5 Hz, 2H, Ar-H). UV-Vis (THF): λ_{max} (ε x 10^{-3})= 468 (83.6), 550 (18.7), 643 nm (12.2). MALDI-TOF (M$^+$): 1370.2; calcd for $C_{85}H_{55}CuN_4O_{11}^+$: 1370.3.

CorLC : Cu^{III} undeca-(4-hydroxyphenyl)corrole (7.2 µmol, 10 mg), compound **1** (22 equiv., 79.2 µmol, 39 mg) and K$_2$CO$_3$ (44 equiv., 158.4

μmol, 22 mg) were added to a round-bottomed flask which was oven dried overnight at 111 °C. The flask was evacuated and backfilled with argon three consecutive times. Dry DMF (5 mL) was then charged by a syringe. The mixture was subsequently stirred at 90 °C for 24 h. After being cooled to room temperature, the solvent was evaporated under reduced pressure. The crude product was purified by chromatography on silica gel (CH_2Cl_2/heptane, 2:1) to yield **CorLC** as a viscous oil (11 mg, 1.6 μmol, 23%). R_f = 0.64 (CH_2Cl_2/Hexane, 2:1). ^{1}H NMR (400 MHz, $CDCl_3$, 25 °C): δ= 6.97 (d, ^3J(H, H) = 8.6 Hz, 3H, Ar-H), 6.83 (t, 8H, Ar-H), 6.61 (brs, 4H, Ar-H), 6.51 (d, ^3J(H, H) = 8.6 Hz, 4H, Ar-H), 6.47 (m, 13H, Ar-H), 6.42 (t, 8H, Ar-H), 6.38 (m, 4H, Ar-H), 6.35 (m, 10H, Ar-H), 6.35 (m, 13H, Ar-H), 6.27 (d, ^3J(H, H) = 8.8 Hz, 4H, Ar-H), 6.17 (d, ^3J(H, H) = 7.5 Hz, 4H, Ar-H), 6.12 (d, ^3J(H, H) = 8.7 Hz, 2H, Ar-H), 4.80 (s, 4H, ArOCH_2Ar), 4.72 (s, 4H, ArOCH_2Ar), 4.70 (s, 4H, ArOCH_2Ar), 4.68 (s, 4H, ArOCH_2Ar), 4.64 (d, 6H, ArOCH_2Ar), 3.80 (m, 44H, OCH_2CH$_2$), 1.68 (m, 44H, OCH$_2$CH_2), 1.38 (m, 44H, OCH$_2$CH$_2$CH_2), 1.25 (m, 352H), 0.86 ppm (m, 66H, CH_3). UV-Vis (CH_2Cl_2): λ_{max} (ε x 10^{-3}) = 464 (124.3), 549 (29.4), 639 nm (17.4). MALDI-TOF (M$^+$): 6417.5 (Maximum iso); calcd for $C_{426}H_{649}CuN_4O_{33}{}^+$: 6417.9 (Maximum iso); ([M+Na]$^+$): 6440.4; calcd for $C_{426}H_{649}CuN_4O_{33}Na^+$: 6440.9.

Notes and references

^{a} Aix Marseille Université, Centrale Marseille, CNRS, iSm2 UMR 7313, 13397, Marseille, France.
^{b} Aix Marseille Université, CNRS, CINaM UMR 7325, 13288, Marseille, France. Fax: (+33) 491 41 8916; E-mails: gabriel.canard@univ-amu.fr and videlot@cinam.univ-mrs.fr
^{c} Department of Inorganic and Analytical Chemistry, University of Geneva, 30 quai Ernest-Ansermet, CH-1211Geneva 4, Switzerland. Fax: (+41) 022 37 960 69; E-mail: emmanuel.terazzi@unige.ch
† Electronic Supplementary Information (ESI) available: supplementary Figures, Tables and Schemes, Analytical data of new compounds. See DOI: 10.1039/b000000x/

1 (a) A. R. Murphy and J. M. J. Frechet, *Chem. Rev.*, 2007, **107**, 1066; (b) J.-H. Chou, M. E. Kosal, H. S. Nalwa, N. A. Rakow and K. S. Suslick, in *The Porphyrin Handbook*, eds. K. M. Kadish, K. M. Smith and R. Guilard, Academic Press, New York, 2000, vol. 6, pp. 43; (c) M. Bouvet, *Anal. Bioanal. Chem.*, 2006, **384**, 366.

2 (a) H. Imahori, T. Umeyama, K. Kurotobi and Y. Takano, *Chem. Commun.*, 2012, **48**, 4032; (b) J. Kesters, P. Verstappen, M. Kelchtermans, L. Lutsen, D. Vanderzande and W. Maes, *Adv. Energy Mater.*, 2015, **5**, 1500218.

3 K. Y. Law, *Chem. Rev.*, 1993, **93**, 449.

4 (a) K. Ohta, H.-D. Nguyen-Tran, L. Tauchi, Y. Kanai, T. Megumi and Y. Takagi, in *Handbook of Porphyrin Science*, eds. K. M. Kadish, K. M. Smith and R. Guilard, 2011, vol. 12, pp. 1; (b) A. Segade, F. López-Calahorra and D. Velasco, *J. Phys. Chem. B*, 2008, **112**, 7395.

5 H. Eichhorn, *J. Porphyrins Phthalocyanines*, 2000, **4**, 88.

6 A. Huijser, T. J. Savenije, A. Kotlewski, S. J. Picken and L. D. A. Siebbeles, *Adv. Mater.*, 2006, **18**, 2234.

7 N. B. Chaure, C. Pal, S. Barard, T. Kreouzis, A. K. Ray, A. N. Cammidge, I. Chambrier, M. J. Cook, C. E. Murphy and M. G. Cain, *J. Mater. Chem.*, 2012, **22**, 19179.

8 (a) D. T. Gryko, *Eur. J. Org. Chem.*, 2002, 1735; (b) S. Nardis, D. Monti and R. Paolesse, *Mini-Rev. Org. Chem.*, 2005, **2**, 355; (c) B. Koszarna and D. T. Gryko, *J. Org. Chem.*, 2006, **71**, 3707; (d) D. T. Gryko, *J. Porphyrins Phthalocyanines*, 2008, **12**, 906; (e) R. Paolesse, *Synlett*, 2008, 2215.

9 (a) J. F. B. Barata, M. G. P. M. S. Neves, A. C. Tomè and J. A. S. Cavaleiro, *J. Porphyrins Phthalocyanines*, 2009, **13**, 415; (b) C. M. Lemon and P. J. Brothers, *J. Porphyrins Phthalocyanines*, 2011, **15**, 809; (c) C. I. M. Santos, J. F. B. Barata, M. J. F. Calvete, L. S. H. P. Vale, D. Dini, M. Meneghetti, M. G. P. M. S. Neves, M. A. F. Faustino, A. C. Tomé and J. A. S. Cavaleiro, *Curr. Org. Synth.*, 2014, **11**, 29.

10 (a) J. P. Collman, M. Kaplun and R. A. Decréau, *Dalton Trans.*, 2006, 554; (b) I. Aviv and Z. Gross, *Chem. Commun.*, 2007, 1987; (c) I. Aviv-Harel and Z. Gross, *Chem. Eur. J.*, 2009, **15**, 8382; (d) I. Nigel-Etinger, A. Mahammed and Z. Gross, *Catal. Sci. Technol.*, 2011, **1**, 578; (e) H.-Y. Liu, M. H. R. Mahmood, S.-X. Qiu and C. K. Chang, *Coord. Chem. Rev.*, 2013, **257**, 1306; (f) K. Nakano, K. Kobayashi, T. Ohkawara, H. Imoto and K. Nozaki, *J. Am. Chem. Soc.*, 2013, **135**, 8456; (g) B. Zyska and M. Schwalbe, *Chem. Commun.*, 2013, **49**, 3799; (h) S. Liu, K. Mase, C. Bougher, S. D. Hicks, M. M. Abu-Omar and S. Fukuzumi, *Inorg. Chem.*, 2014, **53**, 7780.

11 (a) J.-M. Barbe, G. Canard, S. Brandès and R. Guilard, *Angew. Chem. Int. Ed.*, 2005, **44**, 3103; (b) C.-Y. Li, X.-B. Zhang, Z.-X. Han, B. Aakermark, L. Sun, G.-L. Shen and R.-Q. Yu, *Analyst*, 2006, **131**, 388; (c) K. Kurzatkowska, E. Dolusic, W. Dehaen, K. Sieroń-Stołtny, A. Sieroń and H. Radecka, *Anal. Chem.*, 2009, **81**, 7397; (d) V. Blondeau-Patissier, M. Vanotti, T. Prêtre, D. Rabus, L. Tortora, J. M. Barbe and S. Ballandras, *Procedia Eng.*, 2011, **25**, 1085; (e) S. Yang, Y. Wo and M. E. Meyerhoff, *Anal. Chim. Acta*, 2014, **843**, 89.

12 (a) Z. Okun, L. Kupershmidt, M. B. H. Youdim and Z. Gross, *Anti-Cancer Agents Med. Chem.*, 2011, **11**, 380; (b) J. Pohl, I. Saltsman, A. Mahammed, Z. Gross and B. Röder, *J. Appl. Microbiol.*, 2014, **118**, 305; (c) R. D. Teo, H. B. Gray, P. Lim, J. Termini, E. Domeshek and Z. Gross, *Chem. Commun.*, 2014, **50**, 13789; (d) J. F. B. Barata, A. Zamarrón, M. G. P. M. S. Neves, M. A. F. Faustino, A. C. Tomé, J. A. S. Cavaleiro, B. Röder, Á. Juarranz and F. Sanz-Rodríguez, *Eur. J. Med. Chem.*, 2015, **92**, 135.

13 (a) M. Stefanelli, D. Monti, M. Venanzi and R. Paolesse, *New J. Chem.*, 2007, **31**, 1722; (b) A. P. Caricato, M. Lomascolo, A. Luches, F. Mandoj, M. G. Manera, M. Mastroianni, M. Martino, R. Paolesse, R. Rella, F. Romano, T. Tunno and D. Valerini, *Appl. Phys. A*, 2008, **93**, 651; (c) X. Miao, A. Gao, Z. Li, S. Hiroto, H. Shinokubo, A. Osuka and W. Deng, *Appl. Surf. Sci.*, 2009, **255**, 5885; (d) R. van Hameren, J. A. A. W. Elemans, D. Wyrostek, M. Tasior, D. T. Gryko, A. E. Rowan and R. J. M. Nolte, *J. Mater. Chem.*, 2009, **19**, 66; (e) T. Hori and A. Osuka, *Eur. J. Org. Chem.*, 2010, 2379; (f) M. Ding, B. Wang, Z. Wang, J. Zhang, O. Fuhr, D. Fenske and S. Gao, *Chem. Eur. J.*, 2012, **18**, 915; (g) J. F. B. Barata, A. L. Daniel-da-Silva, M. G. P. M. S. Neves, J. A. S. Cavaleiro and T. Trindade, *RSC Adv.*, 2013, **3**, 274; (h) C. I. M. Santos, E. Oliveira, J. Fernández-Lodeiro, J. F. B. Barata, S. M. Santos, M. A. F. Faustino, J. A. S.

Cavaleiro, M. G. P. M. S. Neves and C. Lodeiro, *Inorg. Chem.*, 2013, **52**, 8564; (*i*) B. Bursa, D. Wróbel, K. Lewandowska, A. Graja, M. Grzybowski and D. T. Gryko, *Synth. Met.*, 2013, **176**, 18; (*j*) A. D'Urso, S. Nardis, G. Pomarico, M. E. Fragalà, R. Paolesse and R. Purrello, *J. Am. Chem. Soc.*, 2013, **135**, 8632; (*k*) C. M. Blumenfeld, B. F. Sadtler, G. E. Fernandez, L. Dara, C. Nguyen, F. Alonso-Valenteen, L. Medina-Kauwe, R. A. Moats, N. S. Lewis, R. H. Grubbs, H. B. Gray and K. Sorasaenee, *J. Inorg. Biochem.*, 2014, **140**, 39; (*l*) I. Grabowska, W. Maes, T. H. Ngo, T. Rohand, W. Dehaen, J. Radecki and H. Radecka, *Int. J. Electrochem. Sci.*, 2014, **9**, 1232; (*m*) A. Garai, S. Kumar, W. Sinha, C. S. Purohit, R. Das and S. Kar, *RSC Adv.*, 2015, **5**, 28643; (*n*) R. Orłowski, O. Vakuliuk, M. P. Gullo, O. Danylyuk, B. Ventura, B. Koszarna, A. Tarnowska, N. Jaworska, A. Barbieri and D. T. Gryko, *Chem. Commun.*, 2015, **51**, 8284.

14 (*a*) R. Paolesse, C. Di Natale, A. Macagnano, F. Sagone, M. A. Scarselli, P. Chiaradia, V. I. Troitsky, T. S. Berzina and A. D'Amico, *Langmuir*, 1999, **15**, 1268; (*b*) D. Walker, S. Chappel, A. Mahammed, B. S. Brunschwig, J. R. Winkler, H. B. Gray, A. Zaban and Z. Gross, *J. Porphyrins Phthalocyanines*, 2006, **10**, 1259; (*c*) W. Nulens, I. Grabowska, T. H. Ngo, W. Maes, W. Dehaen, H. Radecka and J. Radecki, *J. Inclusion Phenom. Macrocyclic Chem.*, 2011, **71**, 499; (*d*) L. Tortora, G. Pomarico, S. Nardis, E. Martinelli, A. Catini, A. D'Amico, C. Di Natale and R. Paolesse, *Sens. Actuators B: Chem.*, 2013, **187**, 72; (*e*) W. Sinha, M. Kumar, A. Garai, C. S. Purohit, T. Som and S. Kar, *Dalton Trans.*, 2014, **43**, 12564; (*f*) S.-L. Lai, L. Wang, C. Yang, M.-Y. Chan, X. Guan, C.-C. Kwok and C.-M. Che, *Adv. Funct. Mater.*, 2014, **24**, 4655; (*g*) P. Salvatori, A. Amat, M. Pastore, G. Vitillaro, K. Sudhakar, L. Giribabu, Y. Soujanya and F. De Angelis, *Comput. Theor. Chem.*, 2014, **1030**, 59; (*h*) S. Hamad, G. Krishna Podagatlapalli, M. Ahamad Mohiddon and S. Venugopal Rao, *Chem. Phys. Lett.*, 2015, **621**, 171.

15 I. H. Wasbotten, T. Wondimagegn and A. Ghosh, *J. Am. Chem. Soc.*, 2002, **124**, 8104.

16 (*a*) D. Gao, G. Canard, M. Giorgi and T. S. Balaban, *Eur. J. Inorg. Chem.*, 2012, 5915; (*b*) D. Gao, G. Canard, M. Giorgi, P. Vanloot and T. S. Balaban, *Eur. J. Inorg. Chem.*, 2014, **2014**, 279.

17 (*a*) B. Donnio, B. Heinrich, T. Gulik-Krzywicki, H. Delacroix, D. Guillon and D. W. Bruce, *Chem. Mater.*, 1997, **9**, 2951; (*b*) B. Donnio, D. W. Bruce, H. Delacroix and T. Gulik-Krzywicki, *Liq. Cryst.*, 1997, **23**, 147; (*c*) B. Donnio, K. E. Rowe, C. P. Roll and D. W. Bruce, *Mol. Cryst. Liq. Crys. A*, 1999, **332**, 2893; (*d*) E. Terazzi, S. Torelli, G. Bernardinelli, J.-P. Rivera, J.-M. Bénech, C. Bourgogne, B. Donnio, D. Guillon, D. Imbert, J.-C. G. Bünzli, A. Pinto, D. Jeannerat and C. Piguet, *J. Am. Chem. Soc.*, 2005, **127**, 888.

18 A. Alemayehu, J. Conradie and A. Ghosh, *Eur. J. Inorg. Chem.*, 2011, 1857.

19 S. Berg, K. E. Thomas, C. M. Beavers and A. Ghosh, *Inorg. Chem.*, 2012, **51**, 9911.

20 (*a*) C. Brückner, R. P. Briñas and J. A. Krause-Bauer, *Inorg. Chem.*, 2003, **42**, 4495; (*b*) I. Luobeznova, L. Simkhovich, I. Goldberg and Z. Gross, *Eur. J. Inorg. Chem.*, 2004, 1724; (*c*) A. B. Alemayehu, E. Gonzalez, L. K. Hansen and A. Ghosh, *Inorg. Chem.*, 2009, **48**, 7794; (*d*) D. Bhattacharya, P. Singh and S. Sarkar, *Inorg. Chim. Acta*, 2010, **363**, 4313; (*e*) A. B. Alemayehu, L. K. Hansen and A. Ghosh, *Inorg. Chem.*, 2010, **49**, 7608.

21 S. Sergeyev, W. Pisula and Y. H. Geerts, *Chem. Soc. Rev.*, 2007, **36**, 1902.

22 (*a*) F. Mandoj, S. Nardis, G. Pomarico and R. Paolesse, *J. Porphyrins Phthalocyanines*, 2008, **12**, 19; (*b*) C. Capar, K. E. Thomas and A. Ghosh, *J. Porphyrins Phthalocyanines*, 2008, **12**, 964; (*c*) T. H. Ngo, W. Van Rossom, W. Dehaen and W. Maes, *Org. Biomol. Chem.*, 2009, **7**, 439.

23 B. Donnio, P. García-Vázquez, J.-L. Gallani, D. Guillon, E. Terazzi, *Adv. Mater.*, **2007**, *19*, 3534.

New Journal of Chemistry Accepted Manuscript